

# EFFECTS OF MOVEMENT SPEEDS AND HULL FORMS ON WAVE DRAG REDUCTION IN A SINGLE-FILE SHIP FORMATION

Fengshen Zhu, Zhiming Yuan\*

Department of Naval Architecture, Ocean & Marine Engineering, University of Strathclyde,  
Glasgow, G4 0LZ, UK

fengshen.zhu@strath.ac.uk, zhiming.yuan@strath.ac.uk

**ABSTRACT:** The phenomenon of ducklings following their mothers in a single file configuration has been revealed by the mechanism of wave-riding and wave-passing. The universality of this mechanism is further validated and expanded by a single-file ship formation in present study. A two-ships formation is utilized to investigate the effect of movement speeds and hull form on the wave drag reduction. Based on three objectives, the optimal distances between two ships are determined. It is found that when two ships are in close proximity, the leading vessel experiences a notable decrease in wave drag across most speeds, albeit at the expense of an increase in wave drag for the trailing ship. Once the Froude number surpasses 0.225, the optimal distances between the two ships and their corresponding  $C_{DR}$  values show negligible disparities in minimizing the drag for both the trailing ship and the entire ship formation. Adjusting the main dimensions of the trailing ship can variably affect the total drag of the entire ship formation depending on the objective. Increasing these dimensions may elevate the total drag of the formation when prioritizing the minimization of the leading ship's drag. However, it decreases the total drag when focusing on minimizing the drag of either the trailing ship or the entire ship formation.

## 1. INTRODUCTION

The rationale behind ducklings following their mother to swim in a single-file formation has been unveiled by Yuan et al., shedding lights on the phenomenon from the perspective of wave interference [1]. The small duckling can greatly minimize wave-making resistance by riding the Kelvin waves generated by their mother and even receive a pushing force at an optimal 'sweet point'. From the third one in a row onward, each individual efficiently transfers wave energy to the trailing one without exerting any effort, simply by adjusting their position delicately. Ellingsen pointed out that the benefits of wave riding and wave passing extend beyond just waterfowl, encompassing larger vessels as well [2]. The US Defense Advanced Research Projects Agency (DARPA 2020) has proposed the Sea Trains concept that envisions four or more unmanned surface vehicles sailing in single-file formation or in close lateral and longitudinal formation to minimize collective wave-making resistance [3].

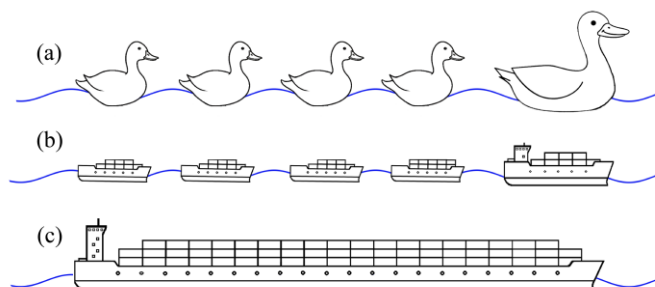


Figure 1. (a) Ducklings following their mother in a single-file formation. (b) Trailing ships following the leading ship in a single-file formation, which is equivalent to (c) a ship with a long parallel mid-body.

To design an optimal ship formation, it is essential to thoroughly consider the intervals between vessels and their speed of movement, as these aspects significantly influence wave interference effects. The optimal spacing and velocity differ based on the configuration's shape, the ships' dimensions, and the total number of ships within the formation. Inspired by the research of Yuan et al. [1], many researchers have studied various ship formations using different methodologies. Ma et al. conducted research into wave drag within a leader-follower ship fleet, utilising the Neumann-Michell potential flow computation [4]. The study concentrated on how the distance between ships and the Froude number affect the follower ship's destructive interference region, where wave drag reduction occurs. Their findings indicated that this interference was ineffective at both low and extremely high Froude numbers. Liu et al. adopted the RANS method to explore hydrodynamic interactions between two KRISO Container Ships and discovered that the resistance of the following ship could be reduced by up to 24.3% [5]. He et al. assessed three ships formations—tandem, parallel, and triangle—at very slow travel speeds [6]. The tandem formation is the most effective for energy preservation, superior to the triangle and parallel formations. To find the optimal positions for each ship in ship formations, Dong et al. developed a hydrodynamic optimization strategy to efficiently reduce energy consumption by automatically adjusting spatial configurations in an echelon formation of unmanned surface vehicles [7]. It was observed that energy-saving efficiency declined from 18.71% to 10.58% when the fleet expanded from two to four ships in optimal formations.

Moreover, multi-hull vessels are specifically engineered to minimise total wave resistance by exploiting the cancellation between waves generated by the hulls [8-10]. Numerical and experimental studies have revealed that, typically, wave interference between the hulls of a catamaran results in a marked increase in total resistance, especially within the range of Froude numbers from 0.45 to 0.65, in comparison to a monohull [11-13]. However, by arranging two hulls in an asymmetric di-hull system and setting the stagger at half the ship's length to induce destructive interference, the overall resistance can be significantly reduced, especially when travelling at speeds close to a Froude number of 0.4 [8,14-16]. In trimaran design, the longitudinal and transverse distance between the main hull and the outriggers are paramount for minimising resistance. Mynard and his colleagues investigated the wave resistance and patterns of Model 9 in the AMECRC series [17]. Utilising the CFD suite SHIPFLOW, slender body theory, and a series of experiments, they identified the optimal longitudinal positions for the outriggers at various operational speeds. Yildiz et al. conducted an analysis of nine distinct outrigger configurations in a trimaran using a three-dimensional RANS solver code [18]. They discovered that when the outriggers are positioned near the aft of the trimaran, the wave interference phenomenon has a beneficial impact on the trimaran's resistance. By integrating the analytical expression of the characteristics of linear wave resistance with the steepest descent method, Wang et al. introduced an efficient method for optimizing the layout of trimaran outriggers [19]. The results demonstrate a high level of accuracy in finding the optimal solution and a significant improvement in computing efficiency when compared to conventional enumeration methods. The concept of Wave Cancellation Multihull (WCM) was proposed by Wilson et al. and examined through experiments [20]. It indicates that, compared to the performance of the twin-hulled SWATH VII, the trainman can achieve a 28% reduction in effective horsepower. Furthermore, Yanuar et al. explored the interference phenomena of quadramarans [21] with hulls arranged in

diamond, tetrahedral, and slice formations, as well as pentamaran ships [22] with asymmetric outrigger configurations.

In this paper, we revisit the wave interference of different ship formations and the multihull ships with different configurations. The effect of the movement speeds on the wave drag reduction of each ship as well as the entire ship formation are investigated, based on three optimal objectives. The effect of hull form on the wave drag is extensively examined by varying the main dimensions of the trailing ship.

## 2. METHODOLOGY

The present research focuses on the wave-making problems, without considering frictional force due to the fluid's viscosity. The fluid domain can be described by using a velocity potential that satisfies Laplace equation. The wave-making resistance and wave patterns are obtained by an in-house code Mhydro [23]. A blunt Wigley hull with  $L/B=5:1$  and  $L/D=10:1$  is adopted in the numerical calculation, where  $L$ ,  $B$ , and  $D$  are ship length, breadth, and draft, respectively. The length of leading and trailing ships are denoted by  $L_0$  and  $L_1$ , respectively.

The wave drag experienced by a single ship represented as  $R_s$  and the wave drag of the  $n$ -th ship moving in a single-file formation is denoted as  $R_n$ . The drag reduction coefficient is defined by

$$C_{DR} = \left(1 - \frac{R_n}{R_s}\right) \times 100\% \quad (1)$$

$C_{DR} > 0$  indicates the wave resistance is reduced in a formation due to the hydrodynamic interaction; whilst  $C_{DR} < 0$  represents an increase in wave resistance. No interaction is found at  $C_{DR} = 0$ , and the wave resistance is the same as that of independent moving. Here,  $n$  denotes the number of ships in the formation, and  $n = 0$  denotes the leading ship.

## 3. ONE LEADING SHIP FOLLOWED BY ONE TRAILING SHIP

When designing an optimal ship formation, three key objectives are considered: minimizing the wave drag on the leading ship, the trailing ships, and the formation as a whole. Each objective may require a distinct optimal distance between the ships. To identify these distances, the gap between two ships is incrementally adjusted while calculating the drag coefficient reduction ( $C_{DR}$ ) values for each configuration. A comparative analysis of these results facilitates the determination of the optimal distances that best meet all three objectives. The optimal distance between two ships is normalized by the length of the leading ship, denoted by  $G_{01}/L_0$ . To investigate the influence of movement speed and hull dimension on wave drag reduction, a simple ship formation, consisting solely of two ships, is employed.

### 3.1 Effect of movement speed on ship resistance

Figure 2(a) compares the wave resistance coefficient  $C_w$  between the present model and Wigley hull III [24], predicted by the MHydro program. The  $C_w$  can be expressed as

$$C_w = \frac{R_w}{\frac{1}{2} \rho U^2 S},$$

where,  $S$  is the area of the wetted body surface,  $U$  is the moving speed and  $\rho$  is the water density. The  $C_W$  curve of the current model exhibits a significantly higher magnitude and more pronounced oscillations compared to those of the Wigley Hull III, which can be attributed to the blunt form of the hull.

Figure 2(b) illustrates the variation in wave drag reduction for the leading ship, the trailing ship, and the fleet, with the objective of minimizing wave drag on the leading ship. When the distance between two ships is reduced to zero, the leading vessel experiences a significant reduction in wave drag at all speeds. However, this advantage comes at the expense of the trailing ship. The  $C_{DR}$  values of the trailing ship are observed to fall below zero, suggesting that it consumes more energy compared to moving independently. Given that the wave resistance of a single vessel moving independently serves as the denominator in the  $C_{DR}$  calculation, it plays a crucial role in influencing the trend of the  $C_{DR}$  values for both the leading and trailing vessels. When the  $C_{DR}$  values of the leading ship rise, those of the trailing ship correspondingly decline, and vice versa. Additionally, as speed increases, the magnitude of these  $C_{DR}$  values tends to diminish.

In Figure 2(b), when the  $Fr$  is below 0.53, the  $C_{DR}$  values of the fleet fall below zero. This indicates that the formation requires increased energy expenditure to reduce the drag on the leading ship. Conversely, when the  $Fr$  exceeds 0.53, these values of the fleet rise above zero. At  $Fr = 0.6$ , this value reaches 22%. Figure 2(e) displays the wave patterns of a single ship and a fleet moving at this speed. At this speed, the wavelength is significantly pronounced, with the ratio of the wavelength to the ship length ( $\lambda/L_0$ ) being 2.26, more than double the length of the ship. Consequently, a wave trough is observed at the stern of the leading ship when it is moving alone. When the two ships are in close proximity, the trailing ship can capitalize on wave riding to reduce its wave drag, whereas the leading ship benefits from an elevated high-pressure zone at its stern.

Figures 2(c) and (d) illustrate variations in wave drag experienced by each individual ship, as well as by the fleet, with the objective of minimizing the wave drag on the trailing ship and the overall formation, respectively. When the Froude number exceeds 0.225, the optimal distances between the ships and their  $C_{DR}$  values exhibit no significant differences when aiming to achieve these two objectives. The leading ship experiences diminished benefits, with its  $C_{DR}$  values approaching zero as the speed increases. The increasing optimal distance between ships with speed, due to the downstream propagation of Kelvin waves, poses a challenge in harnessing wave interference effects. In the  $C_{DR}$  values of the trailing ship or the entire fleet, three distinct peaks are observed at  $Fr = 0.235$ , 0.29, and 0.42, which corresponds to  $\lambda/L_0$  of 0.35, 0.53, and 1.11, respectively. At these specific speeds, the trailing vessel rides approximately 3, 2, and 1 waves, respectively. This allows for sufficient space ahead of the vessel to avoid the wave crests generated by the leading ship, while simultaneously positioning its stern to perfectly align with a wave crest.

However, the optimal distances between two ships for wave drag reduction are significantly different when the  $Fr$  falls below 0.225 in Figure 2(c) and (d). In this range, the optimal gap designed to minimize the wave drag on the trailing ship are wider compared to those aimed at optimizing the drag for the entire formation. Figure 2(f) shows the wave patterns associated with two distinct objectives when the ship formation moves at  $Fr = 0.22$ . The optimal distance for reducing the wave drag on the trailing ship extends by an additional full wavelength compared to the distance aimed at minimizing the wave drag across the entire

formation. By positioning itself one wavelength further back, the trailing ship effectively circumvents the high-pressure zone around its bow, which significantly enhances wave-riding effect. Conversely, advancing one wavelength closer to the leading ship, the trailing vessel sacrifices some of its individual wave-riding benefits in favor of improving the leading ship's condition. This compromise contributes to a reduction in the collective wave resistance experienced by the entire fleet.

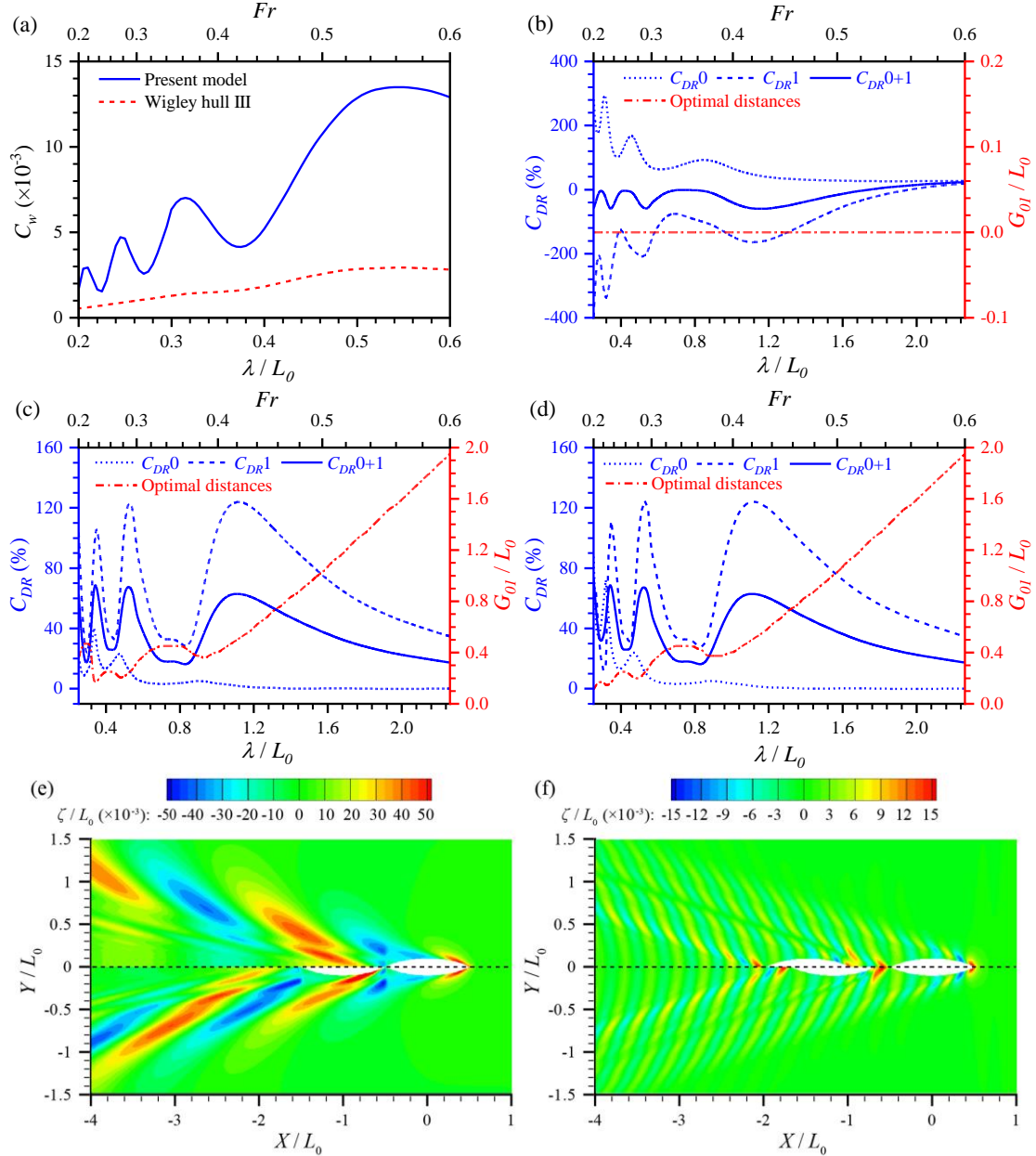


**Figure 2 (a) Comparison of wave drag coefficients between present model and Wigley hull III. (b)~(d) Variations in wave drag of the ship formation and optimal distances between two ships for minimizing the wave drag of the leading ship, the trailing ship, and the wave drag of the whole ship formation, at different movement speeds. (e) The wave patterns of a single ship (upper) and a fleet (lower) moving at  $Fr = 0.6$ . (f) Comparison of wave patterns focuses on the objective of minimizing wave drag for the trailing ship (upper) versus the entire ship formation (lower) at  $Fr = 0.22$ .**

As depicted in Figure 2(c) and (d), when the Froude number exceeds 0.225, the optimal distance between the two ships exhibits an upward, oscillatory pattern as the speed increases. Additionally, the period of oscillation for the optimal distance markedly lengthens with the increase in movement speed. Figure 3 illustrates the progression of optimal distances as the Froude number incrementally rises from 0.285 to 0.385. At  $Fr = 0.285$ , the trailing ship optimizes its wave-riding benefit by strategically positioning its bow in the trough and its stern on the crest of the wave, despite being in proximity to the stern waves generated by the leading ship. As the speed increases and consequently the wavelength extends, the trailing vessel strategically adjusts its position backwards to ensure its stern aligns with the crest of the wave. This adjustment creates an advantageous pressure differential between the bow and stern, facilitating propulsion. This backward maneuvering persists up to a Froude number of 0.325, where the vessel seeks to capitalize on the high-pressure zone present at the wave crest beneath its stern. At  $Fr = 0.345$ , the low-pressure zone near the bow wave of the trailing ship starts to approach the low-pressure zone of the leading ship's stern wave. During this phase, positioning the trailing ship's stern closer to the wave crest becomes increasingly difficult. Subsequently, the trailing vessel initiates a forward movement to optimize the alignment of its bow wave's low-pressure zone with that of the leading ship's stern wave. With the further increase in wavelength, the stern of the trailing ship achieves alignment with a wave crest, significantly enhancing the wave-riding effect. This alignment indicates that the adjustment period for the optimal distance of trailing ships embodies a smooth transition from riding on two waves to engaging with a single wave.

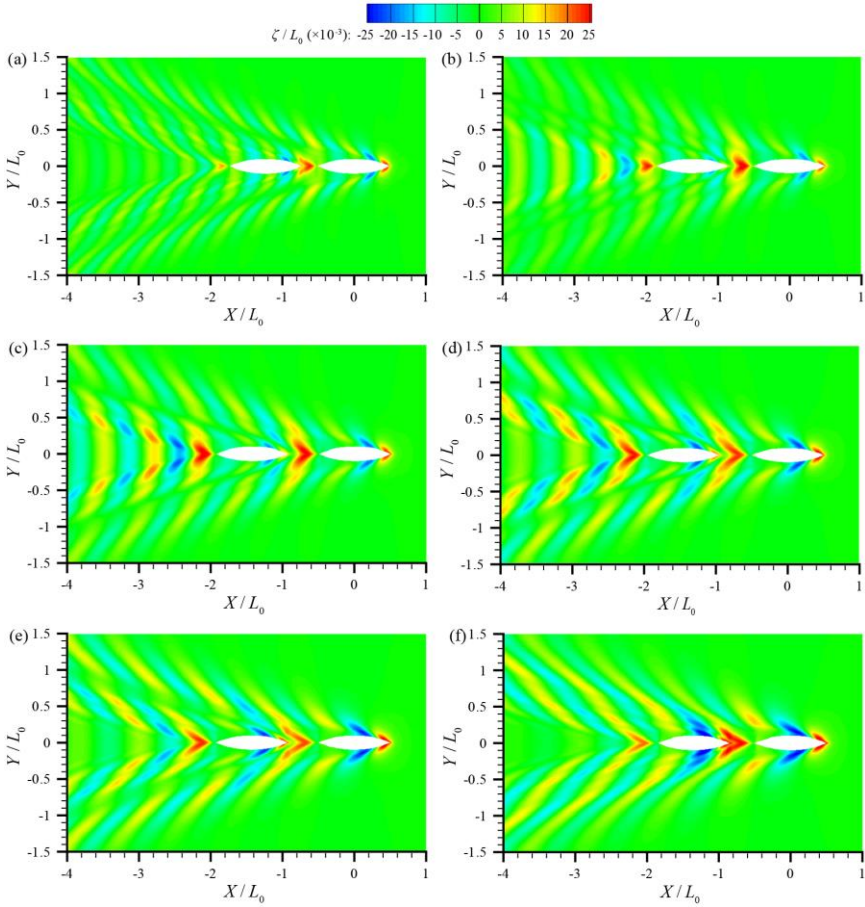


**Figure 3 The wave patterns of a ship formation, when the trailing ship is at its optimal positions for varying Froude numbers (a) 0.285, (b) 0.305, (c) 0.325, (d) 0.345, (e)0.365, (f) 0.385, respectively.**

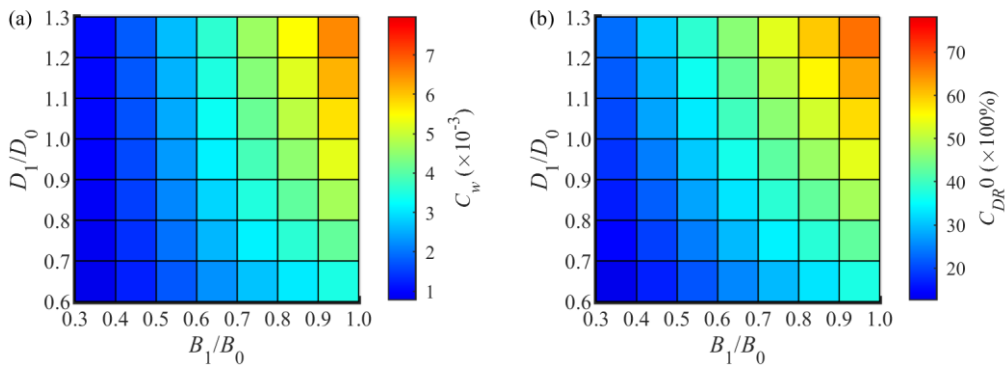
### 3.2 Effect of hull forms on ship resistance

To explore the impact of hull forms of the ship on wave resistance across diverse configurations, the dimensions of the leading ship are held constant with a breadth-to-length ( $B/L$ ) ratio of 1:5 and a draft-to-length ( $T/L$ ) ratio of 1:10. Concurrently, the dimensions of the following vessel, including its breadth and draft (whilst maintaining the same length as the leading ship), are varied. To ensure ships achieve optimal hydrodynamic efficiency, their primary dimensions need to refer to the design specifications. The length-to-beam ( $L/B$ ) ratio is usually maintained within the range of 5.5 to 8.5, whilst the beam-to-draft ( $B/T$ ) ratio commonly ranges from 2.2 to 3.5. In the present study, the dimension ratios for a trailing ship are varied, with the beam ratio ( $B_1/B_0$ ) ranging from 0.3 to 1, and the draft ratio ( $D_1/D_0$ ) set between 0.6 and 1.3. These particular dimension ratios for the trailing ship are crafted to align with the wider hydrodynamic performance standards, ensuring both individual efficiency and cooperative navigational efficacy when in close proximity to or following another vessel.

In single-file ship formations, the alteration in wave drag for each vessel primarily results from the interference of transverse waves, indicating that variations in breadth and draft do not influence the optimal spacing between ships. This investigation concentrates on ship formations of diverse configurations cruising at a Froude number of 0.3, with section 3.1 detailing the optimal distances for various objectives.

Figure 4(a) illustrates the wave resistance  $C_W$  across varying ship breadth and draft ratios. Notably, an upward trend in wave resistance is discernible with increments in the breadth ratio ( $B_1/B_0$ ), indicating that as the ship's breadth increases, so does the wave resistance encountered. Similarly, a positive correlation is evident between wave resistance and the draft ratio ( $D_1/D_0$ ).

Figure 4(b) to (d) show the variations in wave drag reduction for the leading ship, the trailing ship, and the entire fleet, respectively, focused on minimizing the wave drag of the leading vessel. As the breadth and draft of the trailing vessel are augmented, the leading ship gains increasingly significant benefits, with  $C_{DR}$  values up to 80%. However, the trailing ship sacrifices its benefits, even though its  $C_{DR}$  values show an increase trend. The increase of the breadth and draft of the trailing vessel facilitates the formation of the high-pressure between the bow of the trailing ship and the stern of the trailing ship. Simultaneously, the wave resistance of the trailing vessel moving solely increases, resulting in a decrease in its  $C_{DR}$  magnitudes. For the fleet, all  $C_{DR}$  values are negative, indicating an increase in total drag. As the breadth and draft ratios decrease, there is a significant increase in  $C_{DR}$  values, attributed to the leading ship's wave drag becoming progressively more influential over the total drag.



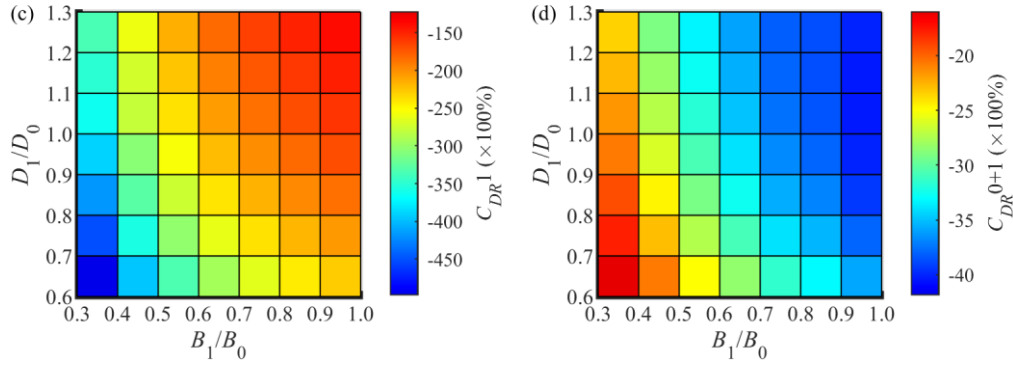


**Figure 4 (a) Wave drag coefficient  $C_W$  across varying ship breadth and draft ratios. (b)~(d) Variations in wave drag reduction for the leading ship, the trailing ship, and the entire fleet, respectively, aiming at minimizing the wave drag of the leading vessel.**

As Section 3.1 points out, when the Froude number exceeds 0.225, the  $C_{DR}$  values become identical for both minimizing the wave drag of the trailing ship and the entire formation. Figure 5(a) to (c) illustrate the variations in wave drag reduction for the leading ship, the trailing ship, and the entire fleet, respectively.

As the breadth and draft of the trailing vessel increase, the  $C_{DR}$  values of the leading ship exhibit a modest upward trend, suggesting that the leading ship harnesses less wave energy from the trailing ship. However, the trailing ship gains significant advantages from riding the waves generated by the leading ship. Even though these  $C_{DR}$  values demonstrate a decreasing trend. For the fleet, the system has the potential to save energy by up to 50%. When the breadth ratio exceeds 0.7 and the draft ratio is greater than 1, the  $C_{DR}$  values approach high level zone. It suggests that when the dimensions of the trailing vessel closely resemble those of the leading vessel, significant reductions in collective wave drag can easily be realized throughout the formation.

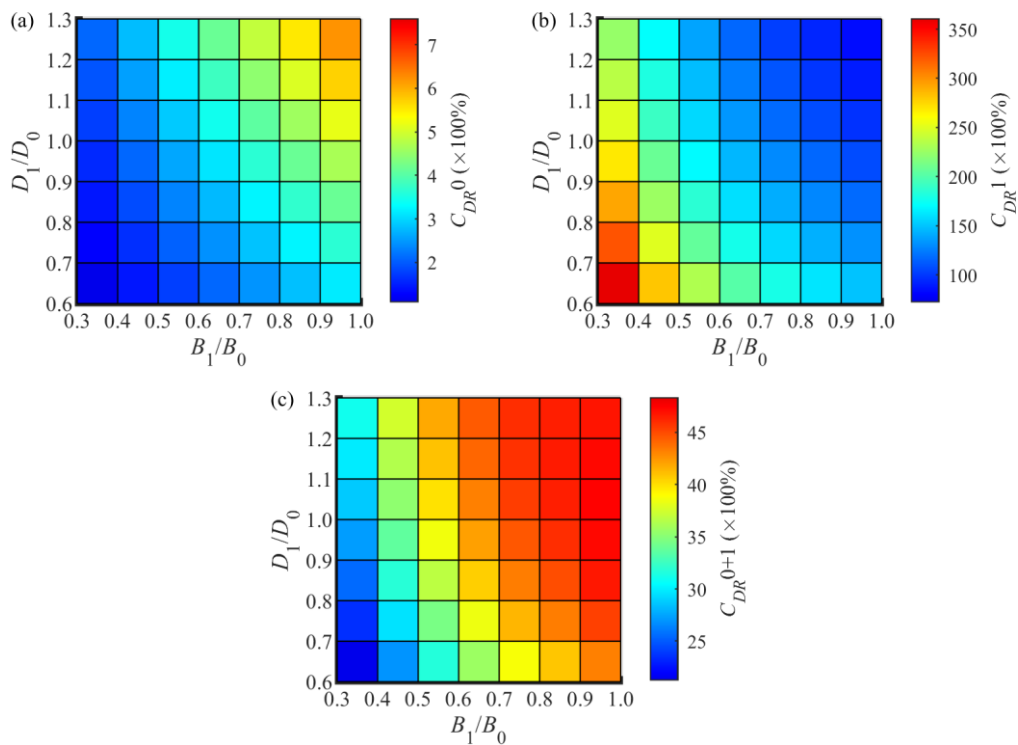


**Figure 5(a)~(c) Variations in wave drag reduction for the leading ship, the trailing ship, and the entire fleet, respectively, aiming at minimizing the wave drag of the trailing vessel or the entire fleet.**

#### 4. CONCLUSIONS

Inspired by ducklings following their mothers in a single-file formation, this study investigates optimal single-file formations, targeting three specific objectives. A formation involving two ships is utilized to explore how the ships' movement speed and main dimensions affect the reduction of wave drag. When the two ships are in close proximity, the leading vessel experiences a significant reduction in wave drag at most of speeds, at the cost of increasing the wave drag of the trailing ship. When the Froude number exceeds 0.225, the optimal distances between two ships and their  $C_{DR}$  values have no differences when aiming to minimize the trailing ship and the whole ship formation. Adjusting the main dimensions of the trailing ship can affect the total drag of the entire ship formation differently depending on the objective. Increasing these dimensions may increase the total drag of the formation when aiming to minimize the drag of the leading ship, but it may decrease the total drag when aiming to minimize the drag of either the trailing ship or the entire ship formation.

#### 5. REFERENCES

- [1] Yuan, Z. M., Chen, M., Jia, L., Ji, C., & Incecik, A. (2021) Wave-riding and wave-passing by ducklings in formation swimming. *Journal of Fluid Mechanics*, 928, R2.
- [2] Ellingsen, S. Å. (2022) Getting the ducks in a row. *Journal of Fluid Mechanics*, 932, F1.
- [3] DARPA, (2020) Sea train, <https://www.darpa.mil/program/sea-train>.
- [4] Ma, C., Zhao, X., Cheng, X., Yang, Y., & Fan, L. (2023). The wave interference and the wave drag of a leader–follower ship fleet. *Ocean Engineering*, 274, 114089.
- [5] Liu, Z., Dai, C., Cui, X., Wang, Y., Liu, H., & Zhou, B. (2023). Hydrodynamic Interactions between Ships in a Fleet. *Journal of Marine Science and Engineering*, 12(1), 56.
- [6] He, Y., Mou, J., Chen, L., Zeng, Q., Huang, Y., Chen, P., & Zhang, S. (2022). Will sailing in formation reduce energy consumption ? Numerical prediction of resistance for ships in different formation configurations. *Applied Energy*, 312, 118695.
- [7] Dong, Z., Liang, X., Guan, X., & Li, W. (2022). Formation optimization of various spacing configurations for a fleet of unmanned surface vehicles based on a hydrodynamic energy-saving strategy. *Ocean Engineering*, 266, 112824.
- [8] Soding, H. (1997). Drastic resistance reduction in catamarans of staggered hulls. *Proceedings of FAST97*.
- [9] Tuck, E. O., & Lazauskas, L. (1998). Optimum hull spacing of a family of multihulls. *Ship Technology Research-Schiffstechnik*, 45(4), 180.
- [10] Yeung, R. W., & Wan, H. (2008). Multihull and surface-effect ship configuration design : a framework for powering minimization.
- [11] Zaghi, S., Broglia, R., & Di Mascio, A. (2011). Analysis of the interference effects for high-speed catamarans by model tests and numerical simulations. *Ocean Engineering*, 38(17-18), 2110-2122.

- [12] Broglia, R., Jacob, B., Zaghi, S., Stern, F., & Olivieri, A. (2014). Experimental investigation of interference effects for high-speed catamarans. *Ocean Engineering*, 76, 75-85.
- [13] He, W., Castiglione, T., Kandasamy, M., & Stern, F. (2015). Numerical analysis of the interference effects on resistance, sinkage and trim of a fast catamaran. *Journal of marine science and technology*, 20, 292-308.
- [14] Yeung, R. W., Poupard, G., Toilliez, J. O., SÖDING, H., Gotman, A. S., & VAN HEMMEN, H. F. (2004). Interference-resistance prediction and its applications to optimal multi-hull configuration design. Discussion. *Transactions-Society of Naval Architects and Marine Engineers*, 112, 142-168.
- [15] Faltinsen, O. M. (2005). *Hydrodynamics of high-speed marine vehicles*. Cambridge university press.
- [16] Yu, D., Lecointre, P., & Yeung, R. W. (2017). Experimentally-based investigation of effects of wave interference on the wave resistance of asymmetric di-hulls. *Applied Ocean Research*, 65, 142-153.
- [17] Mynard, T., Sahoo, P. K., Mikkelsen, J., & McGreer, D. (2008). Numerical and experimental study of wave resistance for trimaran hull forms. *Australian Maritime College, Australia*, 117-132.
- [18] Yildiz, B., Sener, B., Duman, S., & Datla, R. (2020). A numerical and experimental study on the outrigger positioning of a trimaran hull in terms of resistance. *Ocean Engineering*, 198, 106938.
- [19] Wang, S. M., Duan, W. Y., Xu, Q. L., Duan, F., Deng, G. Z., & Li, Y. (2021). Study on fast interference wave resistance optimization method for trimaran outrigger layout. *Ocean Engineering*, 232, 109104.
- [20] Wilson, M. B., Hsu, C. C., & Jenkins, D. S. (1992, June). Experiments and predictions of the resistance characteristics of a wave cancellation multihull ship concept. In *SNAME American Towing Tank Conference* (p. D011S004R001). SNAME.
- [21] Yanuar, Gunawan, Muhyi, A., & Jamaluddin, A. (2016). Ship resistance of quadramaran with various hull position configurations. *Journal of Marine Science and Application*, 15, 28-32.
- [22] Yanuar, Ibadurrahman, Waskito, K. T., Karim, S., & Ichsan, M. (2017). Interference resistance of pentamaran ship model with asymmetric outrigger configurations. *Journal of Marine Science and Application*, 16, 42-47.
- [23] Yuan, Z. M., Kellet, P., Incecik, A., Turan, O., & Boulougouris, E. (2015). Ship-to-ship interaction during overtaking operation in shallow water. *Journal of Ship Research*, 59(03), 172-187.
- [24] Journee, J. M. (1992). Experiments and calculations on four Wigley hullforms. TUDelft, Faculty of Marine Technology, Ship Hydromechanics Laboratory, Report No. 909.